Trapping two types of particles using a double-ring-shaped radially polarized beam

Yaoju Zhang,[1,*] Biaofeng Ding,[1] and Taikei Suyama[2]

[1]*College of Physics and Electronic Information, Wenzhou University, Wenzhou 325035, People's Republic of China*

[2]*Graduate School of Science and Technology, Kumamoto University, Kumamoto 860–8555, Japan*

(Received 16 November 2009; published 24 February 2010)

An optical-trap method based on the illumination of a double-ring-shaped radially polarized beam (R-TEM$^*_{11}$) is proposed. The numerical results based on the vector diffraction theory show that a highly focused R-TEM$^*_{11}$ beam not only can produce a bright spot but also can form an optical cage in the focal region by changing the truncation parameter β, defined as the ratio of the radius of the aperture to the waist of the beam. The radiation forces acting on Rayleigh particles are calculated by using the Rayleigh scattering theory. The bright spot generated by the R-TEM$^*_{11}$ beam with a β value close to 2 can three-dimensionally trap a particle with a refractive index larger than that of the ambient. An optical cage or three-dimensional dark spot generated by the R-TEM$^*_{11}$ beam with a β value close to 1.3 can three-dimensionally trap a particle with refractive index smaller than that of the ambient. Because the adjustment of the truncation parameter can be actualized by simply changing the radius of a circular aperture inserted in the front of the lens, only one optical-trap system in the present method can be used to three-dimensionally trap two types of particles with different refractive indices.

DOI: 10.1103/PhysRevA.81.023831 PACS number(s): 42.25.Fx, 87.80.Cc

I. INTRODUCTION

Polarization that describes the electric-field oscillation direction in electromagnetic waves is an important parameter of laser radiation. A single-ring-shaped radially polarized beam, which is often referred to as a radially polarized R-TEM$^*_{01}$ mode beam, is of particular interest. In the case of high-numerical-aperture (NA) focusing, the R-TEM$^*_{01}$ beam can generate a strong longitudinal electric field at the focal point [1]. This strong longitudinal component forms a tight focal spot that can improve resolution of microscopy [2,3] and enhance laser cutting ability in material processing [4]. Recently, many researchers have demonstrated both in simulation and experiment that radially polarized R-TEM$^*_{01}$ laser beams can be applied in optical-trap systems or as optical tweezers for precise micromanipulation [5–10]. Zhan calculated the radiation forces on metallic Rayleigh particles at the focus using a highly focused ideal R-TEM$^*_{01}$ beam [5]. It was demonstrated by Kawauchi *et al.* [6] and Nieminen *et al.* [7] that R-TEM$^*_{01}$ beams can be used to improve the performance of optical tweezers in the geometrical optics regime and the Mie regime, owing to the reduction of scattering. Yan and Yao [8] demonstrated radiation forces on more general dielectric particles with size ranging from the Rayleigh regime to several wavelengths, illuminated by a highly focused R-TEM$^*_{01}$ beam. Ahluwalia *et al.* investigated experimentally the polarization-induced torque of an R-TEM$^*_{01}$ beam acting on anisotropic microparticles [9]. Analytical calculations by Chen *et al.* [10] showed that the radially polarized R-TEM$^*_{01}$ beams are superior to the linearly polarized beams in the Rayleigh regime in terms of their ability to trap.

It is known that optical-trapping particles can be divided into two types of particles: type A and type B. Type A particles are trapping particles with refractive indices higher than that of the ambient, and type B particles are trapping particles with refractive indices less than that of the ambient. Usually Gaussian beams with the largest intensity at the focus are used to trap the type A particles [11–13]. A highly focused R-TEM$^*_{01}$ beam can generate a sharper bright spot, which is suitable only for the three-dimensional (3D) trap of the type A particles [5–8]. Some weakly focused doughnut-shaped laser beams (such as the Laguerre-Gauss modes and dark hollow beams) can limit the type B particles in two-dimensional (2D) space [14,15]. To trap type B particles in 3D space, the conventional method is to use three doughnut-shaped laser beams orthogonal to each other to form a dark region [16] or to use optical tweezers to generate an optical cage [17]. In this article, we propose a simple 3D optical-trap method, and with this method the type A and type B particles can be trapped by one single-beam optical tweezers. A highly focused double-ring-shaped radially polarized beam (called the R-TEM$^*_{11}$ beam) in our method is used to describe an optical-trap system. The bright spot required for trapping type A particles and the 3D dark spot required for trapping type B particles can be formed, respectively, by simply choosing the truncation parameter of the R-TEM$^*_{11}$ beam rather than adding laser beams.

II. DIFFRACTION OF THE R-TEM$^*_{11}$ BEAM

Generally, there are two types of methods for obtaining an R-TEM$^*_{11}$ beam. One type is to generate the beam directly inside a laser cavity [18], and the other type is to generate the beam outside the laser cavity [19,20]. Figure 1 shows the intensity distribution of an R-TEM$^*_{11}$ beam and the instantaneous polarization state. The appearance of a node in the radial direction implies a phase difference of π between the inner and outer rings, as shown in Fig. 1(b). Thus, when an R-TEM$^*_{11}$ beam is tightly focused, a peculiar behavior of the electric or magnetic field occurs in the focal region because of the interference between the inner and outer rings [21].

According to the vector diffraction theory [21,22], when a radially polarized beam propagating along the z direction is incident on a high-NA lens, the electric field $E(\rho, z)$ and magnetic field $H(\rho, z)$ in the focal region can be obtained

*zhangyaoju@sohu.com

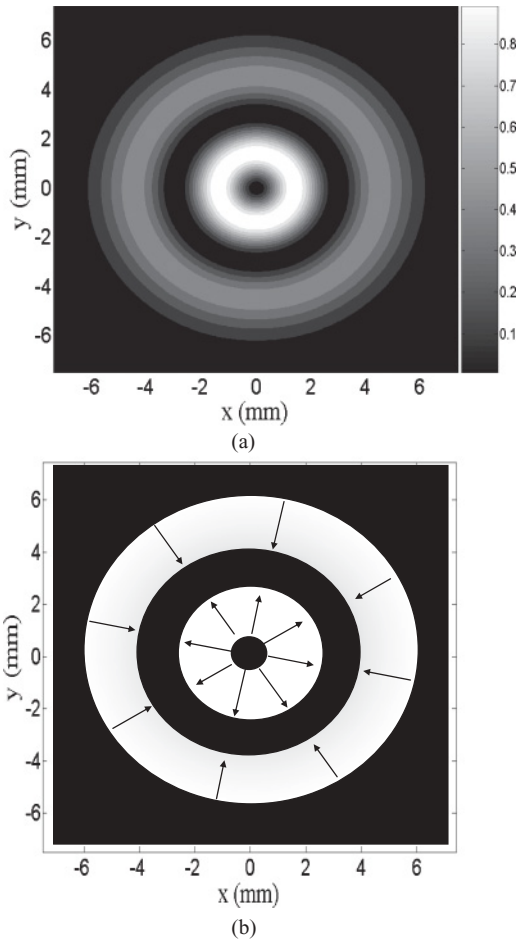

FIG. 1. (a) Intensity distribution and (b) instantaneous polarization state of a radially polarized R-TEM$^*_{11}$ beam with $w = 3$ mm. White and black colors represent the maximum and minimum intensity.

from

$$E_r(\rho, z) = \eta \int_0^\alpha A(\theta)(\sin 2\theta) J_1(k_1 \rho \sin\theta) \exp(ik_1 z \cos\theta) \mathrm{d}\theta, \tag{1}$$

$$E_z(\rho, z) = -2i\eta \int_0^\alpha A(\theta)(\sin^2\theta) J_0(k_1 \rho \sin\theta) \exp(ik_1 z \cos\theta) \mathrm{d}\theta, \tag{2}$$

$$H_\varphi(\rho, z) = \frac{2\eta n_1}{\mu_0 c} \int_0^\alpha A(\theta)(\sin\theta) J_1(k_1 \rho \sin\theta) \exp(ik_1 z \cos\theta) \mathrm{d}\theta, \tag{3}$$

where the azimuthal component of the electric field and the radial and longitudinal components of the magnetic field are zero everywhere in the diffraction field. In Eqs. (1)–(3), α is the convergence angle of the objective, $\eta = E_0 \pi f \sqrt{n_1}/\lambda$, E_0 is the amplitude of electric field in a vacuum, which is related to the power of the incident beam, f is the focal length of the lens, and $k_1 = kn_1 = 2\pi n_1/\lambda$ is the wave number in the immersion liquid with the refractive index n_1. J_n is the nth-order Bessel function of the first kind, and (r, φ, z) are the cylindrical coordinates centered at the geometric focus. $A(\theta)$

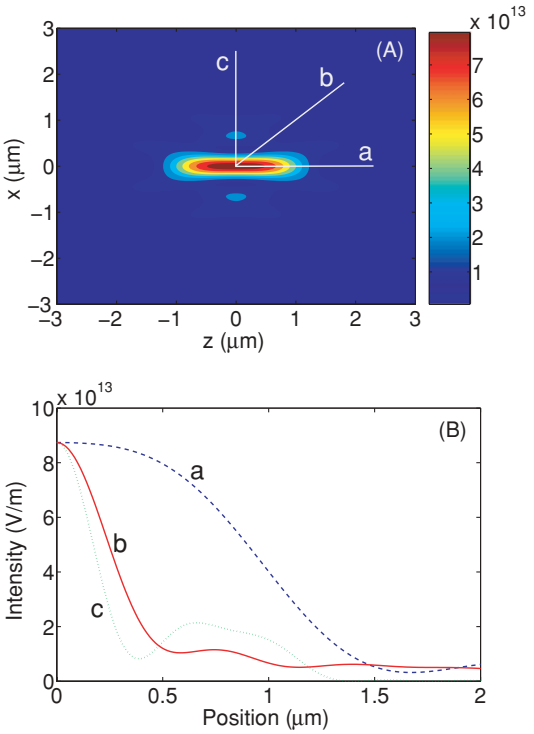

FIG. 2. (Color online) (A) Contours of the total intensity $I(r)$ [$= |E_r(\mathbf{r})|^2 + |E_z(\mathbf{r})|^2$] of the highly focused R-TEM$^*_{11}$ beam in the x–z plane for $\beta = 1.9487$ and (B) intensity profiles in (A) where a, c, and b indicates the z-axis direction, the x-axis direction, and the direction at an angle of 45° with respect to the x axis, respectively.

represents the amplitude and phase distribution at the exit pupil. For an incident R-TEM$^*_{p1}$ beam, $A(\theta)$ can be expressed as [23]

$$A(\theta) = \frac{\beta \sin\theta}{\sin\alpha} \exp\left[-\left(\frac{\beta \sin\theta}{\sin\alpha}\right)^2\right] L_p^1\left[2\left(\frac{\beta \sin\theta}{\sin\alpha}\right)^2\right], \tag{4}$$

where L_p^1 is the generalized Laguerre polynomial with $p+1$ rings and $\beta = R/w$ is called the truncation parameter, where w is the waist of Gauss beam and R is the radius of the aperture inserted in the front of the objective. For a double-ring-shaped radially polarized beam of $p = 1$, β should be larger than 1 because the outer ring of the R-TEM$^*_{11}$ beam will be completely blocked by the pupil if $\beta < 1$.

After some numerical calculations based on MATLAB, we find that when an R-TEM$^*_{11}$ beam is incident on the objective, a 3D bright spot can be formed in the focal region for large or small value of β and a 3D dark spot can be generated when β is close to 1.3. Figure 2(A) shows the contours of the total intensity $I(\mathbf{r})[= |E_r(\rho, z)|^2 + |E_z(\rho, z)|^2]$ in the focal region of a highly focused R-TEM$^*_{11}$ beam in the x–z plane for $\beta = 1.9487$ (90% of laser energy is focused to the focus), and Fig. 2(B) depicts the intensity profiles in (A) where a, c, and b lines indicate the beam propagation direction of $\phi = 0°$, the radial direction of $\phi = 90°$, and the direction of $\phi = 45°$, respectively. Figure 3 displays the contours of the total intensity in the x–z plane when the truncation parameter β is adjusted to 1.3. In calculations, we assume that the numerical

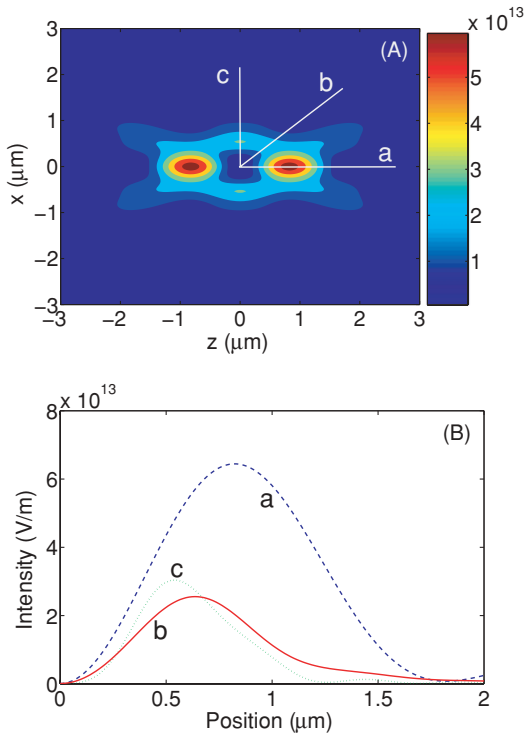

FIG. 3. (Color online) (A) Contours of the total intensity $I(r)$ of the highly focused R-TEM$^*_{11}$ beam in the x–z plane for $\beta = 1.3$ and (B) intensity profiles in (A) where a, c, and b are the same as in Fig. 2. The height of the light wall surrounding the 3D dark spot is highest along the a direction and lowest along the b direction.

aperture of the focusing system is 0.95 n_1. The immersion liquid is water with the refractive index of $n_1 = 1.332$. The laser wavelength is $\lambda = 1.047\,\mu$m, and the laser power is 100 mW. From Fig. 2, it can be seen that when $\beta = 1.9487$, a bright spot is formed in the focal region, which is similar to the focusing property of a highly focused R-TEM$^*_{01}$ beam. Such a bright spot can be used to trap type A particles, which is shown in the next section. However, when $\beta = 1.3$, a 3D dark spot or optical cage can be formed in the focal region, as shown in Fig. 3. The appearance of this peculiar distribution is not shown in the case of R-TEM$^*_{01}$ beam focusing for any values of β. Although the intensity of such an optical cage is not too uniform and the minimum intensity is at the direction of $\phi = 45^\circ$, it can be used to trap type B particles, which is shown in the next section.

III. OPTICAL TRAP FORCES

When a spherical particle of radius a is close to the focus, there are three methods for analysis of optical radiation forces acting on the particle in terms of the particle's size. If $a \ll \lambda$ (generally $a < \lambda/20$), the Rayleigh scattering model is used to determine the radiation forces on such a small particle [24]. If $a \gg \lambda$ (generally $a > 10\lambda$), the ray optics model can be employed as a good approximation to compute the radiation forces [13]. When the particle's dimension is near the wavelength of the incident light, these two models fail to offer an adequate solution to the problem considered. In this case, the generalized Lorenz-Mie theory is used to calculate the radiation force [8,25]. In this article, we assume the radius of particle is much smaller than the wavelength of laser. According to the Rayleigh scattering theory, the gradient force $\boldsymbol{F}_{\text{grad}}$, the absorption force $\boldsymbol{F}_{\text{abs}}$, and the scattering force $\boldsymbol{F}_{\text{scat}}$ can be expressed as [5,26]

$$\boldsymbol{F}_{\text{grad}}(\boldsymbol{r}) = \text{Re}(\gamma)\varepsilon_0 \nabla I(\boldsymbol{r}), \tag{5}$$

$$\boldsymbol{F}_{\text{abs}}(\boldsymbol{r}) = n_1 \langle \boldsymbol{S} \rangle C_{\text{abs}}/c, \tag{6}$$

$$\boldsymbol{F}_{\text{scat}}(\boldsymbol{r}) = n_1 \langle \boldsymbol{S} \rangle C_{\text{scat}}/c, \tag{7}$$

where

$$I(\boldsymbol{r}) = [|E_r(r,z)|^2 + |E_z(r,z)|^2]/4, \tag{8}$$

$$C_{\text{abs}} = k n_1 \text{Im}(\gamma)/\varepsilon_1, \tag{9}$$

$$C_{\text{scat}} = k^4 |\gamma|^2 / 6\pi, \tag{10}$$

$$\langle \boldsymbol{S} \rangle = \{\text{Re}[E_r(r,z) H^*_\varphi(r,z)]\hat{\mathbf{e}}_z - \text{Re}[E_z(r,z) H^*_\varphi(r,z)]\hat{\mathbf{e}}_r\}/2, \tag{11}$$

$$\gamma = 4\pi a^3 \varepsilon_1 (\varepsilon_2 - \varepsilon_1)/(\varepsilon_2 + 2\varepsilon_1). \tag{12}$$

In Eqs. (5)–(12), γ is the polarizability of the particle and ε_2 and ε_1 are the relative permittivities of the particle and the ambient, respectively. C_{abs} and C_{scat} are the absorption and scattering cross sections, respectively. $\langle S \rangle$ is the time-averaged Poynting vector of the focused radially polarized beam, and ε_0 and c are the permittivity and light speed in a vacuum, respectively. Re and Im represent the real and imaginary parts of a complex number, respectively.

The 3D trapping occurs at the focus where all the components of $\boldsymbol{F}_{\text{grad}}$ vanish with a negative derivative. When the Brownian motion of particle is ignored, the condition of a stable trap is that all the components of $\boldsymbol{F}_{\text{grad}}$ at the trapping point are larger than those of the resultant force of $\boldsymbol{F}_{\text{abs}} + \boldsymbol{F}_{\text{scat}}$. Figure 4 shows the calculated gradient forces along the three different directions of a, b, and c shown in Fig. 2(A), acting on a gold particle with an R-TEM$^*_{11}$ beam with $\beta = 1.9487$. Figure 5 displays the calculated gradient forces along the three different directions shown in Fig. 3(A), acting on a air bubble with an R-TEM$^*_{11}$ beam with $\beta = 1.3$. In calculations, we assume the radius of the gold particle is 19.1 nm, and its relative permittivity is $\varepsilon_2 = -54 + 5.9i$ [5], the corresponding refractive index being larger than that of the

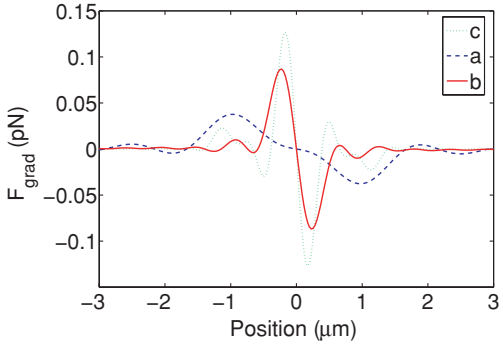

FIG. 4. (Color online) Gradient force F_{grad} acting on a gold particle along the three different directions shown in Fig. 2(A) for the incident R-TEM$^*_{11}$ beam with $\beta = 1.9487$. The radius of the gold particle surrounded by water ($n_1 = 1.332$) is 19.1 nm, and its relative permittivity is $\varepsilon_2 = -54 + 5.9i$.

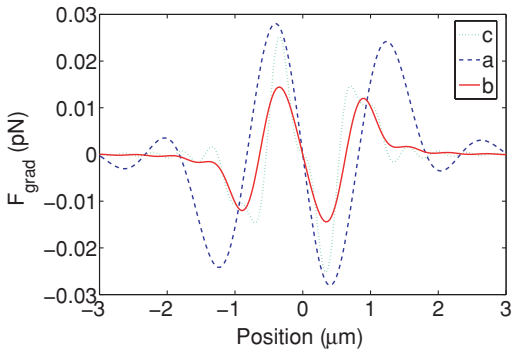

FIG. 5. (Color online) Gradient force F_{grad} acting on an air bubble along the three different directions shown in Fig. 3(A) for the incident R-TEM$^{*}_{11}$ beam with $\beta = 1.3$. The radius of the air bubble surrounded by water is 30 nm, and its refractive index is 1.

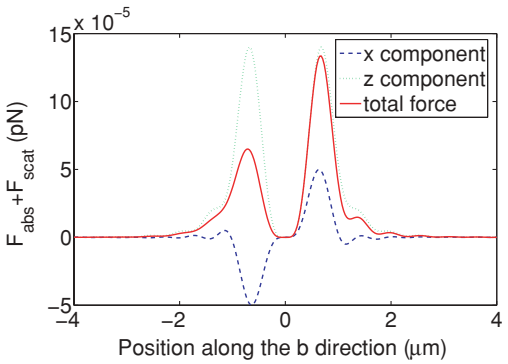

FIG. 7. (Color online) Sum of the absorption and scattering forces $F_{\text{abs}} + F_{\text{scat}}$ acting on a 30-nm (radius) air bubble along the b direction shown in Fig. 3(A) for the incident R-TEM$^{*}_{11}$ beam with $\beta = 1.3$. The dashed, dotted, and solid curves are the transverse component, axial component, and total force along the b direction, respectively.

ambient of $n_1 = 1.332$ (water). The radius of the air bubble is 30 nm, and its refractive index is 1, which is larger than 1.332 of the ambient. The other parameters are same as those used in Fig. 2. From Figs. 4 and 5, it can be seen that the gradient force in the vicinity of the focus has the behavior of a 3D restoring force and thus can draw a particle to the focus in a 3D trap form.

It can be found from Eqs. (1)–(3) that both the electric and magnetic fields are zero in the focal plane and on the optical axis, and consequently the absorption and scattering forces are zero along the a and c directions. Therefore, the trap in the focal plane and on the optical axis is stable for two types of particles with the R-TEM$^{*}_{11}$ beam. We focus our attention on the b direction, in which direction the absorption and scattering forces are strongest. Figures 6 and 7 show the resultant force of the absorption and scattering forces along the b direction for the gold particle and the air bubble, respectively, where the dashed and dotted curves denote the transverse x and axial z components of the resultant force. It can be seen from Figs. 6 and 7 that the axial component is positive, which means that the axial component points along the propagation direction, and the transverse component of the absorption and scattering forces is opposite to the gradient force. In addition,

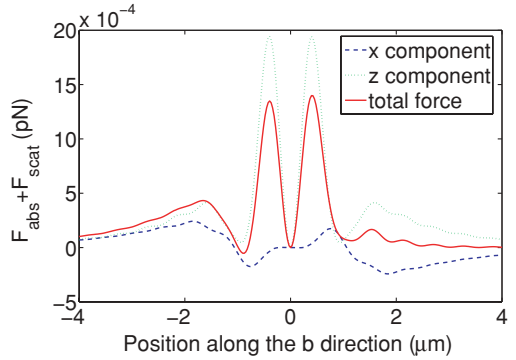

FIG. 6. (Color online) Sum of the absorption and scattering forces $F_{\text{abs}} + F_{\text{scat}}$ acting on a 19.1-nm (radius) gold particle along the b direction shown in Fig. 2(A) for the incident R-TEM$^{*}_{11}$ beam with $\beta = 1.9487$. The dashed, dotted, and solid curves are the transverse component, axial component, and total force along the b direction, respectively.

the magnitude of the axial component is larger than that of the transverse component. To achieve a stable 3D trap, several stability criterion need to be satisfied. The gradient force should be larger than the sum of absorption and scattering forces, that is, $R = F_{\text{grad}}/(F_{\text{abs}} + F_{\text{scat}}) > 1$, where R is called the stability criterion. For a more conservative estimation of R, we use $R = (F_{\text{grad}})_{\text{max}}/(F_{\text{abs}} + F_{\text{scat}})_{\text{max}} > 1$ to estimate the stability. After some calculations, we obtain the trap stabilities of $R = 62$ for the gold particle and $R = 108$ for the air bubble along the b direction. This clearly demonstrates that two types of particles can be stably trapped.

In addition, to form a stable 3D trap, the potential well generated by the gradient forces must be deep enough to overcome the kinetic energy of the trapping particle in Brownian motion. The depth of the well is proportional to the incident intensity, and the steepness and the shape of the potential walls are determined by the intensity gradient $\nabla I(r)$. A generally accepted criterion for the trap stability of a particle is given in terms of the Boltzmann factor as follows [11]:

$$R_{\text{thermal}} \equiv \exp(-U_{\text{m}}/k_B T) \ll 1, \tag{13}$$

where k_B is the Boltzmann constant, T is the temperature of the medium surrounding a particle, and U_{m} is the potential depth given by $|\text{Re}(\gamma)\varepsilon_0 I_{\text{max}}/2|$. For a bright-spot optical trap, U_{m} is determined by the center intensity of the bright spot. However, for a dark-spot optical trap, U_{m} is determined by the maximum intensity along the lowest height direction of the light wall surrounding the dark spot, for example, along the b direction in Fig. 3(A). Assuming a temperature of 300 K, R_{thermal} for the situations considered in Figs. 4 and 5 are calculated to be 1.1×10^{-7} (for the gold particle) and 0.061 (for the air bubble). These results show that these two types of particles can be stably trapped using the R-TEM$^{*}_{11}$ beam with different values of β, although the trap stability parameter of the dark-spot trap for the type B particle is smaller than that of the bright-spot trap for the type A particle. A proper approach to increase the trap stability of type B particles is to improve the uniformity of the light wall surrounding a 3D dark spot [27,28].

IV. CONCLUSION

We have proposed an optical trap method using a double-ring-shaped radially polarized beam. A highly focused R-TEM$_{11}^{*}$ beam not only can produce a bright spot but also can form an optical cage in the focal region by choosing a proper truncation parameter β of the beam. Numerical results show that when β is large enough (for example, $\beta = 1.9487$ in Fig. 4, which means that 90% of the incident laser energy is focused), the type A particles can be trapped, and when β is close to 1.3, the type B particles can be trapped. There are two ways of adjusting the truncation parameter β: one is to change the radius of a circular aperture inserted in the front of the lens and the other is to change the waist size of the beam. In practical trap applications, the way of changing the size of the aperture is simple and convenient. Because the gradient force is much larger than the sum of absorption and scattering forces and because the depth of the potential well generated by the gradient force is larger than the kinetic energy of the trapping particle in Brownian motion, the optical trap using an R-TEM$_{11}^{*}$ beam is stable, which is very useful for the 3D trapping of a strong absorptive particle. The results calculated here suggest the design of an efficient optical trapping device that can trap two types of particles with different refractive indices. We do not doubt that there are many further practical consequences of this concept.

ACKNOWLEDGMENTS

This work was supported by the National Natural Science Foundation of China under Contract 60777005.

[1] K. S. Youngworth and T. G. Brown, Opt. Express **7**, 77 (2000).
[2] S. Quabis, R. Dorn, M. Eberler, O. Glöckl, and G. Leuchs, Opt. Commun. **179**, 1 (2000).
[3] R. Dorn, S. Quabis, and G. Leuchs, Phys. Rev. Lett. **91**, 233901 (2003).
[4] A. V. Nesterov and V. G. Niziev, J. Phys. D **33**, 1817 (2000).
[5] Q. Zhan, Opt. Express **12**, 3377 (2004).
[6] H. Kawauchi, K. Yonezawa, Y. Kozawa, and S. Sato, Opt. Lett. **32**, 1839 (2007).
[7] T. A. Nieminen, N. R. Heckenberg, and H. Rubinsztein-Dunlop, Opt. Lett. **33**, 122 (2008).
[8] S. Yan and B. Yao, Phys. Rev. A **76**, 053836 (2007).
[9] B. P. S. Ahluwalia, X.-C. Yuan, K. J. Moh, and J. Bu, Appl. Phys. Lett. **91**, 171102 (2007).
[10] J. Chen, J. Ng, S. Liu, and Z. Lin, Phys. Rev. E **80**, 026607 (2009).
[11] A. Ashkin, J. M. Dziedzic, J. E. Bjorkholm, and S. Chu, Opt. Lett. **11**, 288 (1986).
[12] D. G. Grier, Nature (London) **424**, 810 (2003).
[13] A. Ashkin, Biophys. J. **61**, 569 (1992).
[14] J. Arlt and M. J. Padgett, Opt. Lett. **25**, 191 (2000).
[15] A. T. O'Neil and M. J. Padgett, Opt. Commun. **185**, 139 (2000).
[16] C. Zhao, L. Wang, and X. Lu, Optik (Stuttgart) **119**, 477 (2008).
[17] S. Kulin, S. Aubin, S. Christe, B. Peker, S. L. Rolston, and L. A. Orozco, J. Opt. B: Quantum Semiclass. Opt. **3**, 353 (2001).
[18] T. Moser, H. Glur, V. Romano, F. Pigeon, O. Parriaux, M. A. Ahmed, and T. Graf, Appl. Phys. B **80**, 707 (2005).
[19] Y. Kozawa and S. Sato, Opt. Lett. **30**, 3063 (2005).
[20] K. Yonezawa, Y. Kozawa, and S. Sato, Opt. Lett. **31**, 2151 (2006).
[21] Y. Kozawa and S. Sato, Opt. Lett. **31**, 820 (2006).
[22] B. Richards and E. Wolf, Proc. R. Soc. A **253**, 358 (1959).
[23] S. Quabis, R. Dorn, M. Eberler, O. Glöckl, and G. Leuchs, Appl. Phys. B: Lasers and Optics **72**, 109 (2001).
[24] Y. Zhang and J. Bai, Opt. Express **17**, 3698 (2009).
[25] J. A. Lock, Appl. Opt. **43**, 2545 (2004).
[26] Y. Harada and T. Asakura, Opt. Commun. **124**, 529 (1996).
[27] N. Bokor and N. Davidson, Opt. Commun. **279**, 229 (2007).
[28] Y. Kozawa and S. Sato, Opt. Lett. **33**, 2326 (2008).